Journal of Proteomics 221 (2020) 103765

Contents lists available at ScienceDirect

Journal of Proteomics

journal homepage: www.elsevier.com/locate/jprot

Proteomic profiling of stallion spermatozoa suggests changes in sperm metabolism and compromised redox regulation after cryopreservation

Francisco E. Martín-Cano[a], Gemma Gaitskell-Phillips[a], José M. Ortiz-Rodríguez[a], Antonio Silva-Rodríguez[b], Ángel Román[c], Patricia Rojo-Domínguez[d], Esmeralda Alonso-Rodríguez[d], José A. Tapia[d], Maria C. Gil[a], C. Ortega-Ferrusola[a], Fernando J. Peña[a,*]

[a] Laboratory of Equine Reproduction and Equine Spermatology, Veterinary Teaching Hospital, University of Extremadura, Cáceres, Spain
[b] Facility of Innovation and Analysis in Animal Source Foodstuffs, University of Extremadura, Cáceres, Spain
[c] Department of Biochemistry and Molecular Biology, University of Extremadura, Badajoz, Spain
[d] Department of Physiology, University of Extremadura, Cáceres, Spain

ARTICLE INFO

Keywords:
Spermatozoa
Proteomics
Horses
Cryopreservation

ABSTRACT

Proteomic technologies allow the detection of thousands of proteins at the same time, being a powerful technique to reveal molecular regulatory mechanisms in spermatozoa and also sperm damage linked to low fertility or specific biotechnologies. Modifications induced by the cryopreservation in the stallion sperm proteome were studied using UHPLC/MS/MS. Ejaculates from fertile stallions were collected and split in two subsamples, one was investigated as fresh (control) samples, and the other aliquot frozen and thawed using standard procedures and investigated as frozen thawed subsamples. UHPLC/MS/MS was used to study the sperm proteome under these two distinct conditions and bioinformatic enrichment analysis conducted. Gene Ontology (GO) and pathway enrichment analysis were performed revealing dramatic changes as consequence of cryopreservation. The terms *oxidative phosphorylation, mitochondrial ATP synthesis coupled electron transport and electron transport chain* were significantly enriched in fresh samples ($P = 5.50 \times 10^{-12}$, 4.26×10^{-8} and $7.26 \times 10^{-8,}$ respectively), while were not significantly enriched in frozen thawed samples ($P = 1$). The GO terms *oxidation reduction process and oxidoreductase activity* were enriched in fresh samples and the enrichment was reduced in frozen thawed samples (1.40×10^{-8}, 1.69×10^{-6} versus 1.13×10^{-2} and 2-86 $\times 10^{-2}$ respectively). Reactome pathways (using human orthologs) significantly enriched in fresh sperm were *TCA cycle and respiratory electron transport* ($P = 1.867 \times 10^{-8}$), *Respiratory electron transport ATP synthesis by chemiosmosis coupling* ($P = 2.124 \times 10^{-5}$), *Citric acid cycle (TCA cycle)*($P = 8.395 \times 10^{-4}$) *Pyruvate metabolism and TCA cycle* ($P = 3.380 \times 10^{-3}$), *Respiratory electron transport* ($P = 2.764 \times 10^{-2}$) *and Beta oxidation of laurolyl-CoA to decanoyl CoA-CoA* ($P = 1.854 \times 10^{-2}$) none of these pathways were enriched in thawed samples (P = 1). We have provided the first detailed study on how the cryopreservation process impacts the stallion sperm proteome. Our findings identify the metabolic proteome and redoxome as the two key groups of proteins affected by the procedure.

Significance: In the present manuscript we investigated how the cryopreservation of stallion spermatozoa impacts the proteome of these cells. This procedure is routinely used in horse breeding and has a major impact in the industry, facilitating the trade of genetic material. This is still a suboptimal biotechnology, with numerous unresolved problems. The limited knowledge of the molecular insults occurring during cryopreservation is behind these problems. The application and development of proteomics to the spermatozoa, allow to obtain valuable information of the specific mechanisms affected by the procedure. In this paper, we report that cryopreservation impacts numerous proteins involved in metabolism regulation (mainly mitochondrial proteins involved in the TCA cycle, and oxidative phosphorylation) and also affects proteins with oxidoreductase activity. Moreover, specific proteins involved in the sperm-oocyte interaction are also affected by the procedure. The information gathered in this study, opens interesting questions and offer new lines of research for the

* Corresponding author at: Veterinary Teaching Hospital, Laboratory of Equine Spermatology and Reproduction, Faculty of Veterinary Medicine University of Extremadura, Avd de la Universidad s/n, 10003 Cáceres, Spain.
E-mail address: fjuanpvega@unex.es (F.J. Peña).

https://doi.org/10.1016/j.jprot.2020.103765
Received 17 January 2020; Received in revised form 25 March 2020; Accepted 26 March 2020
Available online 02 April 2020

improvement of the technology focusing the targets here identified, and the specific steps in the procedure (cooling, toxicity of antioxidants etc.) to be modified to reduce the damage.

1. Introduction

The cryopreservation of spermatozoa is still the most widely used method for long term preservation of male gametes [1–3]. In spite of this, the technology yet has major unresolved questions. Among them the stallion to stallion variability in the quality of the surviving spermatozoa after thawing, and their accelerated senescence. As a consequence, to compensate the reduced sperm lifespan, artificial insemination with cryopreserved spermatozoa requires a very meticulous and costly mare management [1]. In the last decade, intense research has been conducted in stallion sperm biology and in the physiology of spermatozoa under different sperm biotechnologies. The research done has uncovered relevant molecular mechanisms behind these changes [4–11]. Two major areas of research have been the mitochondria and stallion sperm metabolism. These two areas have wide implications in the field of sperm biotechnologies and also in the study of male factor infertility. In stallions, oxidative phosphorylation (OXPHOS) is the principal mechanism for ATP production [6,11]; at the same time the mitochondria are the main source of reactive oxygen species (ROS). In equines, a paradoxical relationship has been discovered with most fertile spermatozoa producing more ROS [11,12]. Moreover, early proteomic studies provide evidences of active β fatty acid oxidation as a source of energy in human and stallion spermatozoa [13,14], moreover this was confirmed through functional experiments in these studies. All these evidences point to a complex and more flexible metabolism in the spermatozoa than that what was initially assumed [13,15]. Mitochondria, in addition to their central role in the cellular metabolism, may control the lifespan of the spermatozoa [16]. The spermatozoa are cells very active after ejaculation and thus their metabolic demands are accentuated [6,16–18]. The development of new strategies to study the sperm proteome using ultra high performance liquid chromatography and mass spectrometry (UHPLC-MS/MS) is rapidly advancing [14,19–22], however to date only one paper has been published reporting proteomic studies in horses [13]. Despite recent research and the importance of this biotechnology, a comprehensive model of the myriad of molecular mechanisms affected by cryopreservation in stallions is still not available. It is evident that proteomic approaches can be a very potent tool to expand our understanding of stallion sperm biology, not only under physiological conditions, but also can be extremely useful for the understanding of stallion infertility and early embryo mortality. The improvement and development of new protocols for conservation of the spermatozoa can also benefit from proteomic studies. Proteomic technologies allow the detection of thousands of proteins at the same time, being a powerful technique to reveal molecular regulatory mechanisms in spermatozoa [20–22]. The aim of the present study was to evaluate changes in the sperm proteome induced by cryopreservation in stallion spermatozoa. Also, in view that recent reports indicate that mitochondria are the organelle more impacted by the process of cryopreservation [5,23,24], special attention was paid to changes in proteins related to metabolism and redox regulation.

2. Material and methods

2.1. Reagents and media

All chemicals were purchased from Sigma-Aldrich (Madrid, Spain), unless otherwise stated.

2.2. Semen collection and processing

Semen was collected from Purebred Spanish horses (PRE) maintained as indicated in specific institutional and European regulations for animal care (Law 6/2913 June 11th and European Directive 2010/63/EU). The ethical committee of the University approved this study. Ejaculates were collected using a warmed and lubricated Missouri model artificial vagina. The gel was removed with an inline filter. Semen was immediately transported to the laboratory after collection for evaluation and processing. The experimental design employed a split sample approach, with single ejaculates divided in two subsamples (fresh and frozen thawed experimental groups). Upon arrival at the laboratory, the semen was processed through colloidal centrifugation [25,26] to remove dead spermatozoa and seminal plasma, and then re-suspended in modified BWW media 95 mM NaCl, 4.7 mM KCl, 1.7 mM CaCl2·2H2O, 1.2 mM KH2PO4, 1.2 mM MgSO4·7H2O, 25 mM NaHCO3, 5.6 mM D-glucose, 275 μM sodium pyruvate, 3.7 μL/mL 60% sodium lactate syrup, 50 U/mL penicillin, 50 μg/mL streptomycin, 20 mM HEPES, and 0.1% (*w/v*) polyvinyl alcohol, 290 and 310 mOsm/kg and pH 7.4 [27](fresh extended semen), or re-suspended in freezing media and frozen using standard procedures that have been previously described by our laboratory (frozen thawed semen) [5], In brief the aliquot was diluted in the freezing medium Cáceres (University of Extremadura Cáceres, Spain) containing 2% egg yolk, 1% glycerol, and 4% dimethylformamide to 100×10^6 spermatozoa/mL. After loading the extended semen into 0.5-mL straws (IMV, L'Aigle, France), the straws were ultrasonically sealed with UltraSeal 21® (Minitube of America MOFA, Verona, Wisconsin, USA) and immediately placed in an IceCube 14S (SY-LAB Neupurkersdorf, Austria) programmable freezer. The following freezing curve was used. Straws were kept for 15 min at 20 °C, and they were then slowly cooled from 20 °C to 5 °C at a cooling rate of 0.1 °C/min. Thereafter the freezing rate was increased to −40 °C/min from 5 °C to −140 °C. The straws were then plunged into liquid nitrogen and stored until analysis. Frozen samples were thawed in a water bath at 37 °C for at least 30 s.

2.3. Experimental design

Three ejaculates from three different stallions were collected and processed as follows. Half of the ejaculate was frozen using standard protocols in our laboratory (Frozen. thawed), the other half was processed as fresh spermatozoa (Fresh). Independent ejaculates from the same stallions were used for sperm functional analysis in fresh and frozen thawed samples.

2.4. Sperm preparation

The spermatozoa (fresh and frozen thawed samples) were washed three times in PBS (600gx 10′) and fresh and FT samples pelleted and kept frozen at −80 °C until analysis The purity of the samples was checked using phase contrast microscopy. Prior to mass spectrometry sample preparation individual samples from each stallion and condition (fresh and frozen thawed) were pooled together, in this way 6 single sperm pools were obtained (Fresh for stallion 1, 2, and 3 and Frozen Thawed for stallion 1, 2, and 3), both fresh and frozen thawed aliquots were obtained from the same stallion and ejaculate.

2.5. Protein solubilization

Isolated spermatozoa (200×10^6 spermatozoa) were solubilized in

lysis buffer (C7:C7Bz0 [3-(4-heptyl) phenyl-(3-hydroxypropyl) dimethylammoniopropanesulfonate], 7 M urea, 2 M thiourea and 40 mM Tris (pH 10.4); 20 µl of lysis buffer was added per each 10×10^6 spermatozoa vortexed and incubated under constant rotation at −4 °C for 1 h.

2.6. Protein quantification

Protein quantification was performed using the 2-D Quant Kit (GE Healthcare, Sevilla Spain) following the instructions of the manufacturer: https://www.gelifesciences.co.jp/tech_support/manual/pdf/80648622.pdf. All samples were normalized to obtain a final concentration of 100 µg of protein per sample.

2.7. In-solution trypsin digestion

200 µL of solution obtained from the previous stage were mixed with 100 µL of 25 mM ammonium bicarbonate buffer pH 8.5 (100 µg of protein in 300 µL of solution). In this solution, the proteins were reduced by adding 30 µL of 10 mM DTT and incubated at 56 °C for 20 min. Then, the proteins were alkylated by adding 30 µL of 20 mM IAA and incubating 30 min at room temperature in the dark. Finally, digestion was performed by adding 1 µL of Trypsin Proteomics Grade (Sigma) (Trypsin solution: 1 µg/µL in 1 mM HCl) during at least 3 h to overnight at 37 °C. Reaction was stopped with 10 µL of 0.1% formic acid and filtered through 0.2 µm (hydrophilic PTFE) to 2 mL dark glass vial. Finally, samples were dried using a nitrogen current with the vial in a heating block at 35 °C. The dry samples were resuspended in 20 µL of buffer A, consisting in water/acetonitrile/formic acid (94.9:5:0.1).

2.8. UHPLC-MS/MS analysis

The separation and analysis of the samples were performed with a UHPLC/MS system consisting of an Agilent 1290 Infinity II Series UHPLC (Agilent Technologies, Santa Clara, CA, USA) equipped with an automated multisampler module and a High Speed Binary Pump, and coupled to an Agilent 6550 Q-TOF Mass Spectrometer (Agilent Technologies, Santa Clara, CA, USA) using an Agilent Jet Stream Dual electrospray (AJS-Dual ESI) interface. The control of the HPLC and Q-TOF were made by the MassHunter Workstation Data Acquisition software (Agilent Technologies, Rev. B.06.01). The sample was injected onto an Agilent AdvanceBio Peptide Mapping HPLC column (2.7 µm, 150 × 2.1 mm, Agilent technologies), thermostatted at 55 °C, at a flow rate of 0.4 mL/min. This column is suitable for peptide separation and analysis. The gradient program started with 2% of B (buffer B: water/acetonitrile/formic acid, 10:89.9:0.1) that stayed 5 min in isocratic mode and then it increased linearly up to 45% B in 40 min, and then it increased up to 95% B in 15 min and it remained constant for 5 min. After this 70 min of run, 5 min of post-time followed using the initial condition for the conditioning of the column for the next run. The mass spectrometer was operated in the positive mode. The nebulizer gas pressure was set to 35 psi, whereas the drying gas flow was set to 10 L/min at a temperature of 250 °C, and the sheath gas flow was set to 12 L/min at a temperature of 300 °C. The capillary spray, fragmentor and octopole RF Vpp voltages were 3500 V, 340 V and 750 V respectively. Profile data were acquired for both MS and MS/MS scans in extended dynamic range mode. MS and MS/MS mass range were 50–1700 *m/z* and scan rates were 8 spectra/s for MS and 3 spectra/s for MS/MS. Auto MS/MS mode was used with precursor selection by abundance and a maximum of 20 precursors selected per cycle. A ramped collision energy was used with a slope of 3.6 and an offset of −4.8. The same ion was rejected after two consecutive scans. Data processing and analysis was performed using Spectrum Mill MS Proteomics Workbench (Rev B.04.01, Agilent Technologies, Santa Clara, CA, USA). Briefly, raw data were extracted under default conditions as follows: non fixed or variable modifications were selected; [MH] + 50–10,000 *m/z*; maximum precursor charge +5; retention time and m/z tolerance ± 60 s; minimum signal-to-noise MS (S/N) 25; finding ^{12}C signals. The MS/MS search against the appropriate and updated protein database (in this case: Uniprot/Horse) was performed with the following criteria: non fixed modifications were selected and as variable modification: carbamidomethylated cysteines was selected; tryptic digestion with 5 maximum missed cleavages; ESI-Q-TOF instrument; minimum matched peak intensity 50%; maximum ambiguous precursor charge +5; monoisotopic masses; peptide precursor mass tolerance 20 ppm; product ion mass tolerance 50 ppm; and calculation of reversed database scores. Validation of peptide and protein data was performed using auto thresholds with a %FR (false discovery rate) at 1.2%. The result of protein was obtained like protein summarized using all validations; score > 4 and % SPI (Scored Peak Intensity: the percentage of the extracted spectrum that is explained by the database search result) 60.

2.9. Sperm proteome analysis

The proteins identified in fresh and frozen thawed samples were queried for gene ontology (GO) terms (http://geneontology.org) and classified according to a) cellular component (CC), b) biological process (BO) and c) molecular function (MF) according to the PANTHER classification system (PANTHER v.14.0) (http://www.pantherdb.org), and g:Profiler (https://biit.cs.ut.ee/gprofiler/gost) against the *Equus caballus* database (https://www.uniprot.org/uniprot/?query=Equus+caballus&sort=score) following detailed published protocols [28–30]. The lists of proteins were queried against the equine proteome database for significant enrichment using the Fisher's exact test corrected with a False Discovery Rate (FDR) set at $P < .05$.

2.10. Analysis of metabolic and redox proteomes

PANTHER pathways (http://www.pantherdb.org/pathway/pathwayList.jsp) and KEGG pathways (https://www.genome.jp/kegg/) [31–34] analysis were used to identify biological pathways likely to be active in stallion spermatozoa and its changes after cryopreservation. The significance of the presence of the protein list was queried against the equine genome database using the Fisher's exact test and a FDR < 0.05; g:Profiler was also used to perform an enrichment analysis of changes induced by cryopreservation in the stallion sperm proteome using the multiquery option that allows to compare two sets of proteins ordered by the FDR value [30]. Visualization of the enrichment analysis was done using Cytoscape v 3.7.1 (https://cytoscape.org) and EnrichmentMap (http://apps.cytoscape.org/apps/enrichmentmap) as described in [35]. Due to the increased deep of the human proteome in terms of annotation, we transformed the equine annotations to their human orthologs using g:Profiler (https://biit.cs.ut.ee/gprofiler/orth) and we performed again a pathway enrichment analysis and visualization using g:Profiler and Cytoscape, in this way pathways analysis using Reactome (https://reactome.org) and WiKipathways (https://www.wikipathways.org/index.php/WikiPathways) were also performed.

2.11. Changes in the relative amounts of proteins after cryopreservation

Qlucore Omics Explorer (Lund, Sweden https://qlucore.com) was used to compare changes in the relative amounts of proteins based in spectral counts between fresh and frozen thawed aliquots. Differences were considered significant when $P < .05$. Results are displayed as means ± SEM. Data were Log2 transformed and normalized, and an ANOVA two-groups (fresh vs frozen and thawed) comparison was performed filtered by fold change (> 2) with $P < .05$ and FDR < 0.05.

2.12. Western blotting (WB)

SDS-PAGE was performed to separate the proteins according to their

apparent molecular masses, as previously described [36,37]. Briefly, proteins were extracted and denatured by boiling for 10 min at 70 °C in a loading buffer supplemented with 5% mercaptoethanol. The protein content was calculated using the Bradford assay [38]. Ten micrograms of sperm protein extract were loaded on a 10% polyacrylamide gel and resolved using SDS-PAGE. Immunoblotting was performed by incubating the membranes with blocking buffer containing primary antibodies (SOD2, AKAP4, ATP5A1 from Biorbit, Cambridge UK, orb11395, orb538389 and orb375551, OGDH, Cell Signaling, Danver Massachusetts, USA #26865) following the instructions of the manufacturers overnight at 4 °C. Secondary antibodies were used at 0.27 μg/mL (anti-mouse) or 0.16 μg/mL (anti-rabbit) depending on the primary antibody used. Positive controls used were SH-SY5Y cells for AKAP4, Brain lysates for OGDH and Atp5a1, and lung lysates for SOD2.

2.13. Computer-assisted sperm analysis (CASA)

Sperm motility and velocity were assessed with Computer-assisted Sperm Analysis (CASA) system (ISAS Proiser, Valencia, Spain) [26,37]. Samples were loaded in a Leja® chamber with a depth of 20 μm (Leja, Amsterdam, The Netherlands) and placed on a warmed stage at 37 °C. Then 60 consecutive digitized images obtained using a 10× negative phase-contrast objective (Olympus CX 41) and 500 spermatozoa per sample were analyzed in random fields. Spermatozoa VAP > 35 μm/s were considered motile. Spermatozoa deviating < 45% from a straight line were classified as linearly motile. The following parameters were measured: percentages of linear motile spermatozoa, and circular (VCL) straight line (VSL) and average (VAP) velocities in μm/s.

2.14. Flow cytometry determination of GSH, viability and mitochondrial membrane potential

Intracellular GSH was determined using protocols [39,40],optimized for GSH detection in flow cytometry [41] validated for equine spermatozoa in our laboratory [17]. The mitochondrial membrane potential and sperm viability were also simultaneously assessed. In brief, sperm aliquots (1–5 × 10^6 sperm/mL) were stained with JC-1 1 μM, monochlorobimane (MCB) 10 μM, (20 min in the dark at r.t.) and DRAQ7 3 μM (10 min in the dark at r.t). MCB was detected at peak excitation of 405 nm and emission of 450/45 nm BP, JC-1 was detected as a peak excitation of 511 nm and emission of 596 nm (aggregates) and DRAQ7, peak excitation 640, and emission at 690 nm. Analyses were conducted using a Cytoflex® flow cytometer (Beckman Coulter) equipped with violet, blue, yellow and red lasers. Files were exported as FCS files and analyzed using FlowjoV 10.6.1 Software (Ashland, OR, USA). Unstained, single-stained, and Fluorescence Minus One (FMO) controls were used to determine compensations and positive and negative events, as well as to set regions of interest as described in previous publications from our laboratory [42–44]. Both 2D plots and computational analysis were performed. For computational analysis, data from all the replicates for each treatment were concatenated and single cell events analyzed. Flow cytometry data were analyzed using non-linear dimensionally reduction techniques (t-SNE) [45,46], allowing automatic gating of cells as previously described for sperm analysis [23,47].

2.15. Measurement of oxidation-reduction potential

Oxidation-reduction potential was measured using the RedoxSYS® Diagnostic system (Englewood CO, USA) [48] following previous published protocols from our laboratory [16]. In brief, 30 μL of spermatozoa were loaded in the sample port of the pre-inserted disposable sensor, and the measurement began at the moment of loading. After 4 min, the static oxidative-reduction potential (sORP) is provided in millivolts (mV). ORP is calculated with the Nernst equation $ORP = E^o - RT/nF \ln[Red]/[Ox]$, being E^o = standard reduction potential, R = universal gas constant, T = absolute temperature, n = number of moles of exchanged electrons, F = Faraday constant, [Red] = concentration of reduced species, [Ox] = concentration of oxidized species [49]. According to the manufacturer, sORP is measured while applying a low oxidizing current (1 nA) to the sample. After allowing 1 min and 50 s for equilibration, the reader measures twice per second over 10 s. the difference in potential between the working and reference electrode in mV. As controls, we used seminal plasma (rich in antioxidants) [50–56], and samples treated with 800 μM SO_4Fe and 200 μM H_20_2 to induce the Fenton Reaction [57].

2.16. Statistical analysis

The normality of the data was assessed using the Kolmogorov-Smirnoff test. Paired *t*-tests and One-way ANOVA followed by Dunnett's multiple comparisons test were performed using GraphPad Prism version 7.00 for Mac, La Jolla California USA, (www.graphpad.com).

3. Results

3.1. Identification of sperm proteins in fresh and frozen thawed stallion spermatozoa

2226 different proteins were identified in stallion spermatozoa, of these 2180 were aligned to the equine proteome database. The complete lists of proteins is given as supplementary material (Suppl Table 1) and as a Data in Brief article. The Data set has been deposited to the ProteomeXchange Consortium via [58] the PRIDE partner repository with the dataset identifier PRIDE PXD018111.

3.2. Cryopreservation impacts the stallion sperm proteome

3.2.1. Gene ontology

Gene Ontology (GO) analysis of biological processes of stallion sperm proteins obtained from fresh spermatozoa, returned enriched terms related to metabolism (Table 1). Molecular function GO terms overrepresented were: *Pyruvate dehydrogenase (NAD+) activity, proton*

Table 1
Panther overrepresentation test of proteins of interest identified by UHPLC/MS/MS and gene ontology analysis of fresh equine (*Equus caballus*) spermatozoa.

GO Biological process	Fold enrichment	*P* value
Acetyl-CoA biosynthetic process from pyruvate (GO:0006086)	30.0	3.21E-02
Acetyl-CoA biosynthetic process (GO 0006085)	22.91	1.16E-02
Sperm capacitation (GO:0048240)	16.80	1.16E-03
Sperm-egg recognition (GO:0035036)	15.75	3.02E-04
Binding of sperm to zona pellucida (GO:0007339)	13.36	2.45E-02
ATP synthesis coupled proton transport (GO:0015986)	12.78	3.15E-02
Energy coupled proton transport, down electrochemical gradient (GO:0015985)	12.78	3.25E-02
Cell-cell recognition (GO:0009988)	12.19	1.85E-03
Citrate metabolic process (GO:0006101)	12.00	9.59E-03
Tricarboxylic acid cycle (GO:0006099)	11.76	4.98E-02
Pyruvate metabolic process (GO:0006090)	11.14	1.02E-05
Tricarboxylic acid metabolic process (GO:0072350)	10.84	1.83E-02
Mitochondrial ATP synthesis coupled electron transport (GO:0042775)	10.77	1.07E-03
ATP synthesis coupled electron transport (GO:0042773)	10.74	2.60E-04
ATP biosynthetic process (GO:0006754)	10.68	9.16E-07
Aerobic respiration (GO:0009060)	9.88	1.38E-04
Oxidative phosphorylation (GO:0006119)	9.63	6.84E-04

Panther overrepresentation Test (Released 20190711); GOntology database (GO Ontology database Released 2019-07-03), Fisher's test, FDR $P < .05$.

Table 2
Panther overrepresentation test of proteins of interest identified by UHPLC/MS/MS and gene ontology analysis of frozen thawed equine (*Equus caballus*) spermatozoa.

GO Biological process	Fold enrichment	*P* value
Cognition (GO:0050890)	3.52	1.34E-05
Microtubule-based process (GO:0007017)	2.55	1.41E-06
Cytoskeleton organization (GO:0007010)	2.77	1.05E-06
Organelle organization (GO:0006996)	1.61	5.74E-06

Panther overrepresentation Test (Released 20190711); GOntology database (GO Ontology database Released 2019-07-03), Fisher's test, FDR P < .05.

transport ATP synthase activity, rotational mechanism, and cytochrome c oxidase activity. GO terms enriched in frozen thawed samples are given in Table 2. We did a direct comparison of GO terms for biological processes between fresh and frozen thawed samples using g:Profiler. The terms *oxidative phosphorylation, mitochondrial ATP synthesis coupled electron transport and electron transport chain* were significantly enriched in fresh samples (Fig. 1A) ($P = 5.50 \times 10^{-12}$, 4.26×10^{-8} and $7.26 \times 10^{-8,}$ respectively), while were not significantly enriched in frozen thawed samples ($P = 1$) (Fig. 1B). The GO terms *oxidation reduction process and oxidoreductase activity* were enriched in fresh samples and the enrichment was reduced in frozen thawed samples (1.40×10^{-8}, 1.69×10^{-6} versus 1.13×10^{-2} and 2.86×10^{-2} respectively) (Fig. 1A-B).

3.2.2. *PANTHER, KEGG and reactome pathways*

Moreover, and to further clarify cellular functions enriched in stallion spermatozoa and changes after cryopreservation, PANTHER cellular pathways and KEGG analysis, were performed. The PANTHER pathways overrepresented in fresh aliquots were *Pyruvate metabolism* (Fold enrichment 16.6, $P = 2.51E-04$, FDR 1.37E-02) and *Glycolysis* (Fold enrichment 9.96 $P = 7.36E-05$, FDR 6.03E-03). The KEGG overrepresented pathways were *Oxidative phosphorylation, metabolic pathways, carbon metabolism, glycolysis/gluconeogenesis, citrate cycle (TCA*

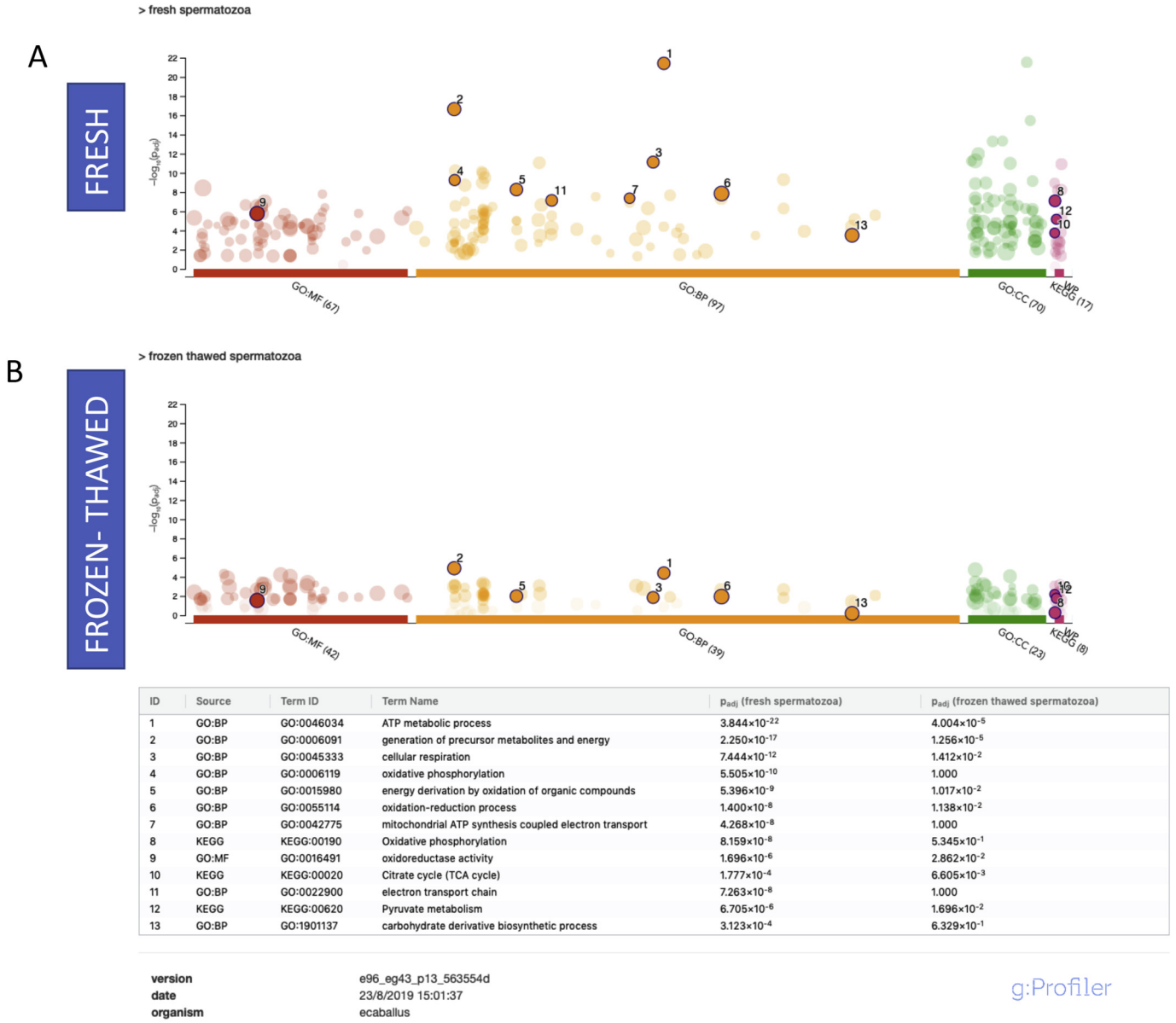

ID	Source	Term ID	Term Name	p_{adj} (fresh spermatozoa)	p_{adj} (frozen thawed spermatozoa)
1	GO:BP	GO:0046034	ATP metabolic process	3.844×10^{-22}	4.004×10^{-5}
2	GO:BP	GO:0006091	generation of precursor metabolites and energy	2.250×10^{-17}	1.256×10^{-5}
3	GO:BP	GO:0045333	cellular respiration	7.444×10^{-12}	1.412×10^{-2}
4	GO:BP	GO:0006119	oxidative phosphorylation	5.505×10^{-10}	1.000
5	GO:BP	GO:0015980	energy derivation by oxidation of organic compounds	5.396×10^{-9}	1.017×10^{-2}
6	GO:BP	GO:0055114	oxidation-reduction process	1.400×10^{-8}	1.138×10^{-2}
7	GO:BP	GO:0042775	mitochondrial ATP synthesis coupled electron transport	4.268×10^{-8}	1.000
8	KEGG	KEGG:00190	Oxidative phosphorylation	8.159×10^{-8}	5.345×10^{-1}
9	GO:MF	GO:0016491	oxidoreductase activity	1.696×10^{-6}	2.862×10^{-2}
10	KEGG	KEGG:00020	Citrate cycle (TCA cycle)	1.777×10^{-4}	6.605×10^{-3}
11	GO:BP	GO:0022900	electron transport chain	7.263×10^{-8}	1.000
12	KEGG	KEGG:00620	Pyruvate metabolism	6.705×10^{-6}	1.696×10^{-2}
13	GO:BP	GO:1901137	carbohydrate derivative biosynthetic process	3.123×10^{-4}	6.329×10^{-1}

version	e96_eg43_p13_563554d
date	23/8/2019 15:01:37
organism	ecaballus

g:Profiler

Fig. 1. g:GOST multiquery Manhattan plot showing comparative enrichment analysis of stallion sperm proteins obtained from the same ejaculate under two different experimental conditions (fresh and frozen thawed). Gene Ontology terms (GO) for molecular function (MF) are in red, for Biological Process (BP) in orange, for cellular component (CC) in green. The *P* values are depicted in the y axis and more detailed in the result table below the image.

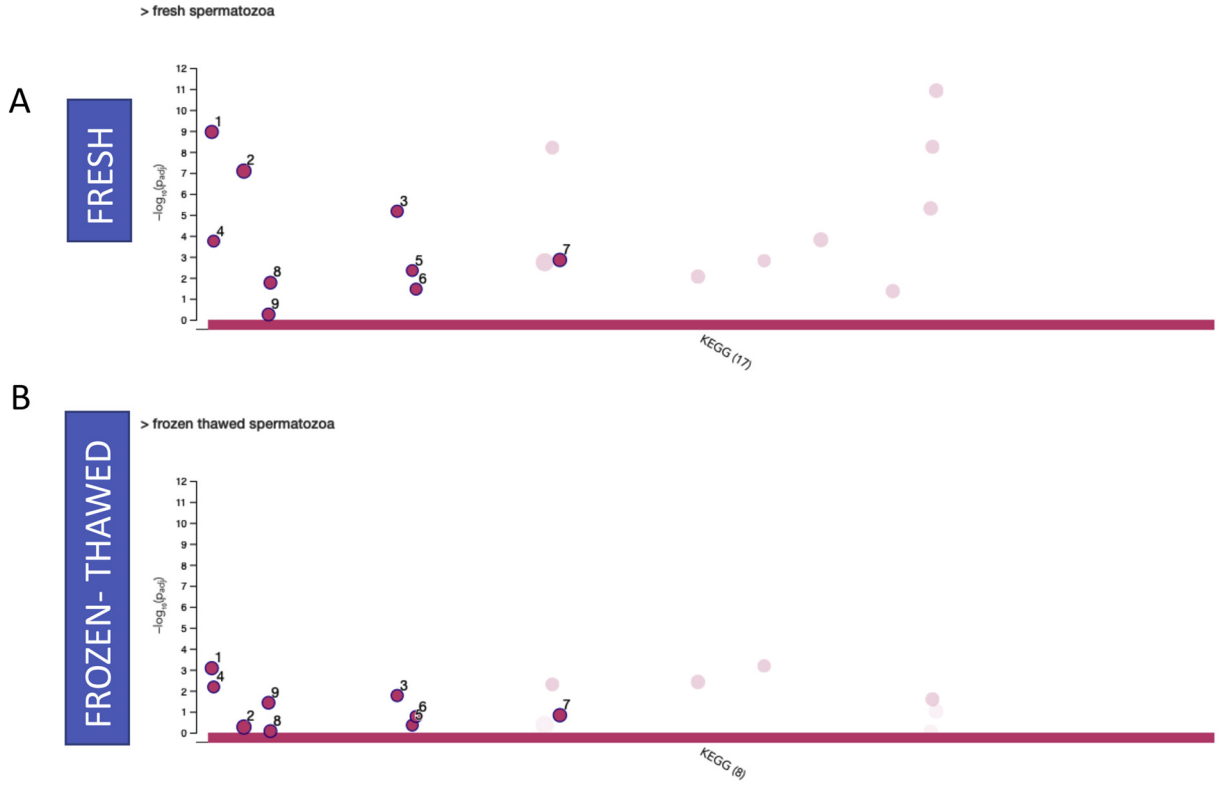

ID	Source	Term ID	Term Name	p_{adj} (fresh spermatozoa)	p_{adj} (frozen thawed spermatozoa)
1	KEGG	KEGG:00010	Glycolysis / Gluconeogenesis	1.113×10^{-9}	8.430×10^{-4}
2	KEGG	KEGG:00190	Oxidative phosphorylation	8.159×10^{-8}	5.345×10^{-1}
3	KEGG	KEGG:00620	Pyruvate metabolism	6.705×10^{-6}	1.696×10^{-2}
4	KEGG	KEGG:00020	Citrate cycle (TCA cycle)	1.777×10^{-4}	6.605×10^{-3}
5	KEGG	KEGG:00630	Glyoxylate and dicarboxylate metabolism	4.510×10^{-3}	4.379×10^{-1}
6	KEGG	KEGG:00640	Propanoate metabolism	3.453×10^{-2}	1.690×10^{-1}
7	KEGG	KEGG:01230	Biosynthesis of amino acids	1.405×10^{-3}	1.467×10^{-1}
8	KEGG	KEGG:00280	Valine, leucine and isoleucine degradation	1.708×10^{-2}	8.351×10^{-1}
9	KEGG	KEGG:00270	Cysteine and methionine metabolism	5.565×10^{-1}	3.735×10^{-2}

version	e96_eg43_p13_563554d
date	24/8/2019 15:27:03
organism	ecaballus

g:Profiler

Fig. 2. g:GOST multiquery Manhattan plot showing comparative enrichment analysis of stallion sperm proteins obtained from the same ejaculate under two different experimental conditions (fresh and frozen thawed). Kyoto Encyclopedia of Genes and Genomes (KEGG) pathways are depicted in red. The *P* values are depicted in the y axis and more detailed in the result table below the image.

cycle), pyruvate metabolism, propaonate metabolism, valine, leucine and isoleucine degradation, fatty acid degradation, tryptophan metabolism, butaonate metabolism, biosynthesis of amino acids, fatty acid metabolism, and cysteine and methionine metabolism.

In frozen thawed aliquots no significant enrichment was detected on PANTHER pathways, while KEGG pathway analysis retrieved the term *Glycolysis/Gluconeogenesis* with 10 proteins present and a FDR < 0.05. Using g: Profiler for direct comparison between fresh and frozen thawed samples provided KEGG enriched pathways, and after transformation of the equine proteins to their human orthologs provided Reactome and Wiki enriched pathways (Fig. 3). The principal KEGG pathways enriched in fresh samples were *Glycolysis /Gluconeogenesis* ($P = 1.11 \times 10^{-9}$) *oxidative phosphorylation* ($P = 8.16 \times 10^{-8}$), *Pyruvate metabolism* ($P = 6.795 \times 10^{-6}$) *and Citrate cycle* ($P = 1.777 \times 10^{-4}$), in Frozen thawed samples *oxidative phosphorylation* was no longer ($P = .5345$) present and *glycolysis/gluconeogenesis* and the *Citrate cycle* were still present but with lower significance ($P = 8.430 \times 10^{-4}$ and 6.605×10^{-3} respectively). Interestingly the pathway *Cysteine and methionine metabolism* appeared enriched only in frozen thawed samples ($P = .037$) (Fig. 2).

Reactome pathways (using human orthologs) significantly enriched in fresh sperm were *TCA cycle and respiratory electron transport* ($P = 1.867 \times 10^{-8}$), *Respiratory electron transport ATP synthesis by chemiosmosis coupling* ($P = 2.124 \times 10^{-5}$), *Citric acid cycle (TCA cycle)* ($P = 8.395 \times 10^{-4}$) *Pyruvate metabolism and TCA cycle* ($P = 3.380 \times 10^{-3}$), *Respiratory electron transport* ($P = 2.764 \times 10^{-2}$) *and Beta oxidation of laurolyl-CoA to decanoyl CoA-CoA* ($P = 1.854 \times 10^{-2}$), none of these pathways were enriched in frozen thawed samples (P = 1). WiKi pathways enriched in fresh samples were *Electron Transport Chain (OXPHOS system in mitochondria)* ($P = 1.048 \times 10^{-4}$), *Fatty Acid Beta Oxidation* ($P = 4.331 \times 10^{-4}$), *glycolysis and gluconeogenesis* ($P = 7.110 \times 10^{-4}$) *and Oxidative phosphorylation* ($P = 2.056 \times 10^{-3}$), that were no longer present in the frozen thawed aliquots (P = 1)(Fig. 3).

3.2.3. Cryopreservation impact in sperm protein classes

PANTHER was also applied to identify overrepresented classes of proteins. The classes of proteins overrepresented in fresh stallion spermatozoa are presented in Table 3 and Fig. 4. Three groups of overrepresented proteins were detected in the frozen thawed aliquots,

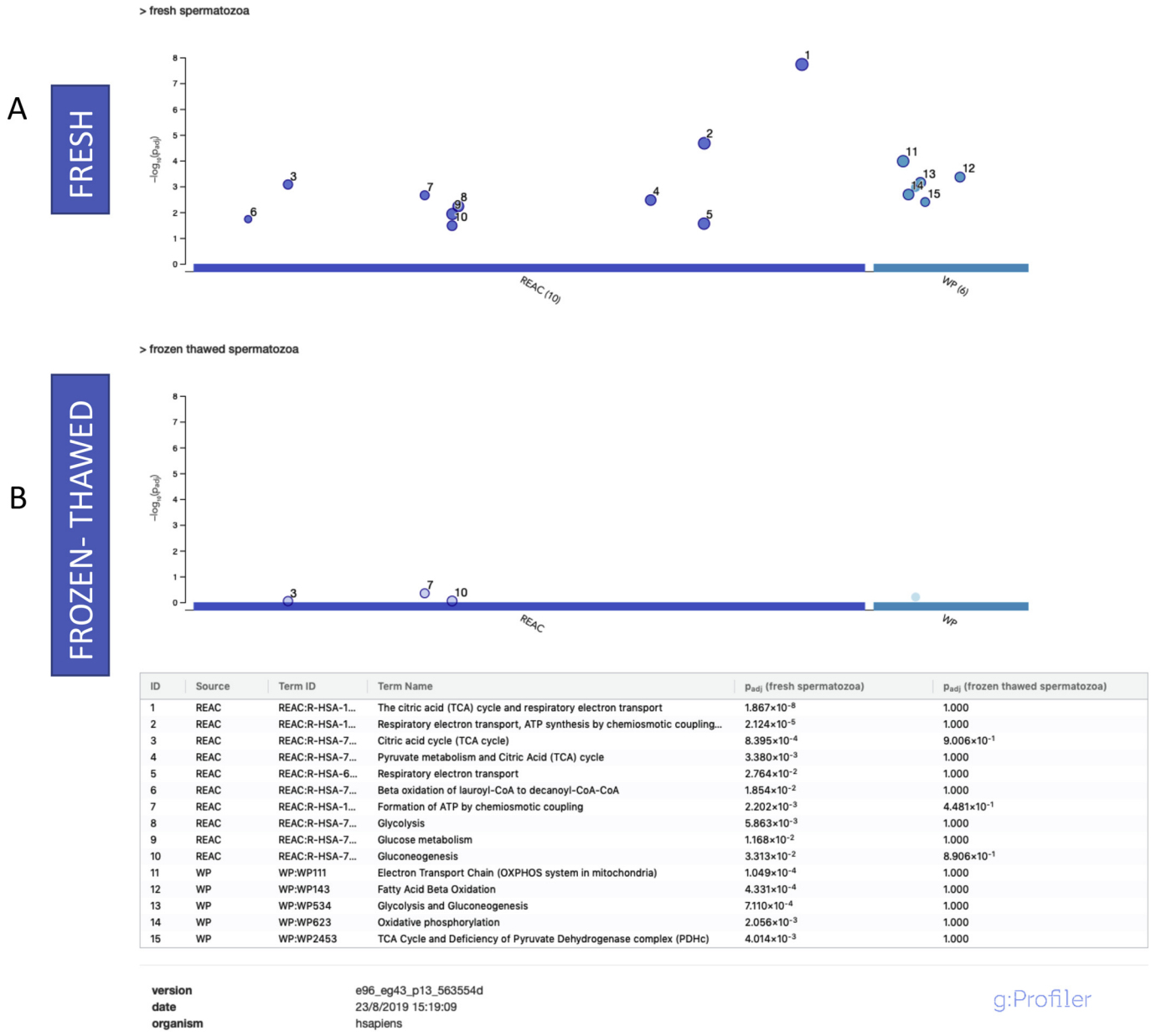

ID	Source	Term ID	Term Name	p_{adj} (fresh spermatozoa)	p_{adj} (frozen thawed spermatozoa)
1	REAC	REAC:R-HSA-1...	The citric acid (TCA) cycle and respiratory electron transport	1.867×10^{-8}	1.000
2	REAC	REAC:R-HSA-1...	Respiratory electron transport, ATP synthesis by chemiosmotic coupling...	2.124×10^{-5}	1.000
3	REAC	REAC:R-HSA-7...	Citric acid cycle (TCA cycle)	8.395×10^{-4}	9.006×10^{-1}
4	REAC	REAC:R-HSA-7...	Pyruvate metabolism and Citric Acid (TCA) cycle	3.380×10^{-3}	1.000
5	REAC	REAC:R-HSA-6...	Respiratory electron transport	2.764×10^{-2}	1.000
6	REAC	REAC:R-HSA-7...	Beta oxidation of lauroyl-CoA to decanoyl-CoA-CoA	1.854×10^{-2}	1.000
7	REAC	REAC:R-HSA-1...	Formation of ATP by chemiosmotic coupling	2.202×10^{-3}	4.481×10^{-1}
8	REAC	REAC:R-HSA-7...	Glycolysis	5.863×10^{-3}	1.000
9	REAC	REAC:R-HSA-7...	Glucose metabolism	1.168×10^{-2}	1.000
10	REAC	REAC:R-HSA-7...	Gluconeogenesis	3.313×10^{-2}	8.906×10^{-1}
11	WP	WP:WP111	Electron Transport Chain (OXPHOS system in mitochondria)	1.049×10^{-4}	1.000
12	WP	WP:WP143	Fatty Acid Beta Oxidation	4.331×10^{-4}	1.000
13	WP	WP:WP534	Glycolysis and Gluconeogenesis	7.110×10^{-4}	1.000
14	WP	WP:WP623	Oxidative phosphorylation	2.056×10^{-3}	1.000
15	WP	WP:WP2453	TCA Cycle and Deficiency of Pyruvate Dehydrogenase complex (PDHc)	4.014×10^{-3}	1.000

version	e96_eg43_p13_563554d
date	23/8/2019 15:19:09
organism	hsapiens

g:Profiler

Fig. 3. g:GOST multiquery Manhattan plot showing comparative enrichment analysis of stallion sperm proteins obtained from the same ejaculate under two different experimental conditions (fresh and frozen thawed). Reactome (REAC) and wiki (WK) pathways pathways (using human orthologs) are depicted in dark and light blue respectively. The *P* values are depicted in the y axis and more detailed in the result table below the image.

microtubule binding motor protein (Fold Enrichment 4.34 $P = 6.19e\text{-}06$ FDR 1.333–02), *microtubule family cytoskeletal p*roteins (Fold Enrichment 2.65 $P = 8.25E\text{-}05$ FDR 8.90E-03,) and *cytoskeletal proteins* (Fold enrichment 1.98, $P = 1.00E\text{-}04$, FDR 7.19E-03) (Fig. 5).

3.2.4. Changes in the relative proportion of proteins after cryopreservation

Changes in the relative proportion of proteins as consequence of cryopreservation were compared. Cryopreservation caused reduction in the relative abundance of 58 proteins and increase in 86 proteins ($P < .05$). Changes are presented as heat maps of proteins with reduced relative abundance in frozen thawed samples and proteins with increased relative abundance expression in the frozen thawed aliquot (Fig. 6). Interestingly proteins related to *oxidative phosphorylation, pyruvate metabolism, and citrate cycle were reduced after cryopreservatio*n. Also the abundance of key antioxidant proteins were reduced in frozen thawed aliquots, like *Superoxide dismutase [Mn] mitochondrial or the aldehyde dehydrogenase 2 family member;* also the relative abundance of proteins related to recognition, binding and penetration of the oocyte were reduced in frozen thawed aliquots including *Zona pellucida binding protein and the IZUMO family member 4* (Fig. 6). When a principal component analysis (PCA) was performed, the dramatic impact of cryopreservation on the sperm proteome was clearly revealed (Fig. 7). A subset of these proteins was further validated using western identification (Fig. 8).

3.2.5. Cryopreservation impacts sperm viability, motility and velocities, impairs mitochondrial membrane potential and reduces intracellular GSH

Freezing a thawing caused an important reduction in the percentages of total and linear motile spermatozoa ($P < .001$) (Fig. 9 A B). Sperm velocities were also reduced after freezing and thawing ($P > .001$) (Fig. 9C-E). Viability and GSH content dropped significantly after freezing and thawing (Fig. 9 F-G) ($P < .01$). The sperm parameter more impacted by the process of cryopreservation was mitochondrial function, with a dramatic reduction in the percentage of

Table 3
Panther overrepresentation test of proteins classes of interest identified by UHPLC/MS/MS and gene ontology analysis of equine (*Equus caballus*) spermatozoa.

PANTHER Protein Class	Fold Enrichment	Raw P value	FDR
Chaperonin (PC00073)	18.86	2.49E-05	1.07E-03
ATP synthase (PC00002)	7.11	3.68E-04	1.13E-02
Microtubule binding motor protein (PC00156)	4.95	3.77E-04	1.01E-02
Oxidase (PC00175)	4.52	6.78E-05	2.43E-03
Chaperone (PC00072)	4.24	4.71E-04	1.12E-02
Microtubule family cytoskeletal protein (PC00157)	3.92	1.24E-06	2.66E-04
Dehydrogenase (PC00092)	3.84	1.09E-05	5.88E-04
Oxidoreductase (PC00176)	2.78	2.81E-06	3.02E-04
Cytoskeletal protein (PC00085)	2.55	1.02E-05	7.28E-04

Panther overrepresentation test (Released 20190711) Panther version 14.1 Released 2019-02-12 Test Type: FISHER. Correction: FDR.

spermatozoa showing high mitochondrial membrane potential ($P < .001$) (Fig. 9H I). Computational cytometry revealed an overall reduction of mitochondrial activity in the whole population of spermatozoa as revealed by the t-SNE maps of fresh and frozen thawed spermatozoa (Fig. 9 *J*-K).

3.2.6. Frozen thawed spermatozoa are in a higher oxidation -reduction potential that fresh spermatozoa

Overall oxidation reduction of spermatozoa significantly changed after cryopreservation; with frozen thawed samples more oxidized than fresh samples. The fresh spermatozoa presented an sORP of $6.1 \pm 0.3\,mV/10^6$ spermatozoa while frozen thawed spermatozoa had a sORP of $8.6 \pm 0.3\,mV/10^6$ spermatozoa ($P < .001$) (Fig. 9 L).

3.2.7. Biological network exploration of the stallion sperm metabolic proteome

In view that metabolic annotations were dominant in the stallion sperm proteome, g:Profiler and Cytoscape were used to investigate the functional network of sperm proteins involved in metabolic processes (Fig. 10). The analysis was performed using Reactome pathways using human orthologs of the sperm proteins. Interestingly, metabolism of lipids appeared to be prevalent in stallion spermatozoa, including the β-oxidation of very long fatty acids. In the metabolism of carbohydrates is relevant the presence of the Pentose phosphate pathway, and in the metabolism of amino acids and derivatives the carnitine synthesis, glutathione synthesis and recycling and glutathione conjugation.

4. Discussion

In this study, we investigated the proteome of the stallion spermatozoa in fresh and frozen thawed split subsamples from the same ejaculate. We payed special attention to the metabolic and redox proteome. Gene ontology and enrichment network analysis revealed a profound impact in the stallion sperm proteome as consequence cryopreservation. This paper offers new molecular insights into the damage that spermatozoa experience after freezing and thawing, and interestingly, goes well in line with recent research pointing to sperm metabolism and redox regulation as key elements in the understanding of sperm biology. Moreover, this is to the best of our knowledge, the first report on the effect of cryopreservation on the stallion sperm proteome.

Among the protein classes predominant in fresh stallion spermatozoa were ATP synthases and oxidoreductases. Gene ontology and pathway analysis also revealed the predominance of mitochondrial proteins. Analysis of functional networks also revealed the enrichment in oxidative phosphorylation and metabolic pathways of lipids, carbohydrates and amino acids. Interestingly none of the proteins above mentioned were enriched after cryopreservation.

Simultaneous g:Profiler enrichment analysis revealed profound changes in the proteome after cryopreservation, GO ontology terms for biological functions revealed the dramatic reduction in proteins involved in oxidative phosphorylation, and reduced enrichment in other GO terms related to metabolism (Fig. 1). These findings reinforce the theory that the mitochondria are specially compromised as consequence of cryopreservation as seen in the functional analysis in our study, and are in the origin of the accelerated senescence of spermatozoa surviving freezing and thawing [6,16,18,23,24,27,59–61]. Also, enrichment analysis of pathways confirmed that the stallion sperm metabolism and redox proteome are dramatically impacted by cryopreservation. The enrichment analysis based in KEGG pathways revealed that only the pathways *glycolysis/gluconeogenesis and Citrate Cycle* were still present in thawed samples, although with lower significance, after cryopreservation. These results were further confirmed after transformation of the equine proteins into their human orthologs, and then Reactome and Wikipathways analysis was conducted. In this case, is worth mentioning that no pathway was present in thawed

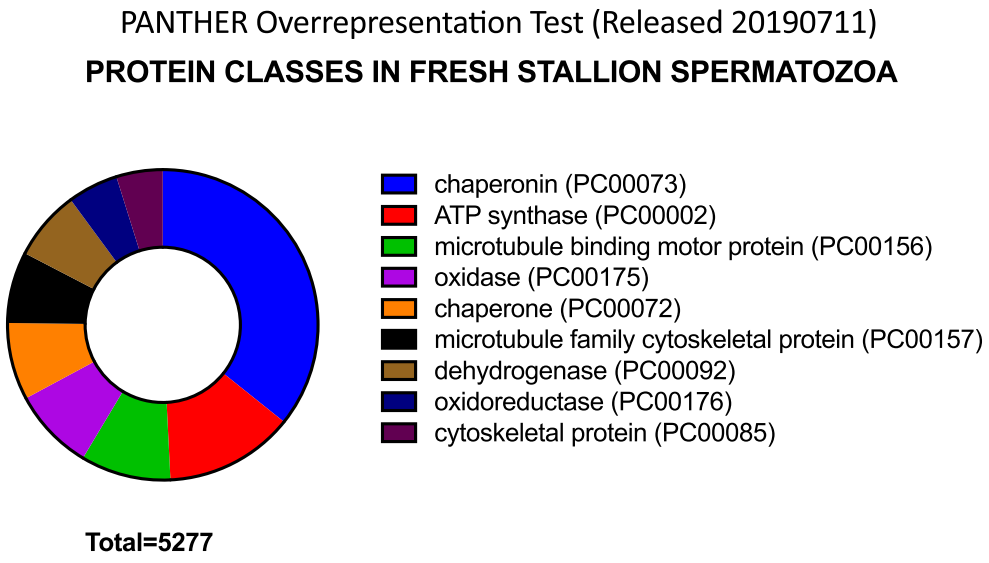

Fig. 4. Panther overrepresentation test of proteins classes of interest identified by UHPLC/MS/MS and gene ontology analysis of equine (*Equus caballus*) spermatozoa. Detailed P values for each protein class are given in Table 3.

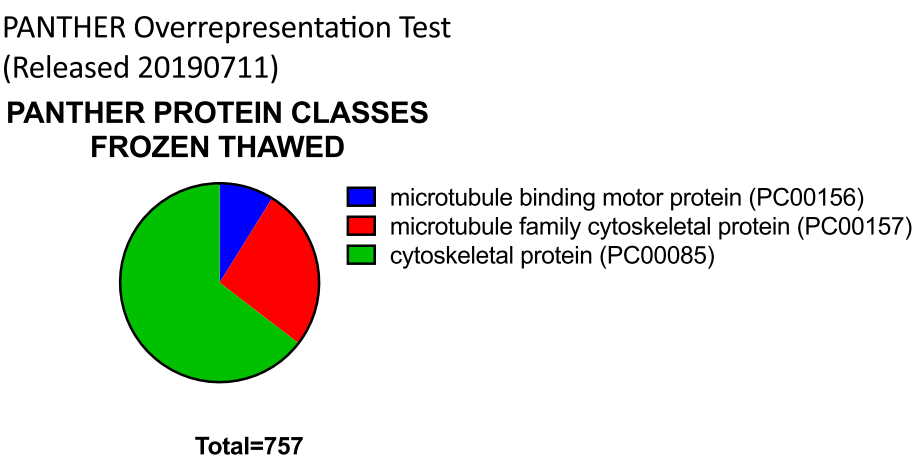

Fig. 5. Panther overrepresentation test of proteins classes of interest identified by UHPLC/MS/MS and gene ontology analysis of frozen thawed equine (*Equus caballus*) spermatozoa. Three groups of overrepresented proteins were detected in the frozen thawed aliquot, *microtubule binding motor protein* (Fold Enrichment 4.34 $P = 6.19e\text{-}06$ FDR 1.333–02), *microtubule family cytoskeletal* proteins (Fold Enrichment 2.65 $P = 8.25E\text{-}05$ FDR 8.90E-03,) and *cytoskeletal proteins* (Fold enrichment 1.98, $P = 1.00E\text{-}04$, FDR 7.19E-03).

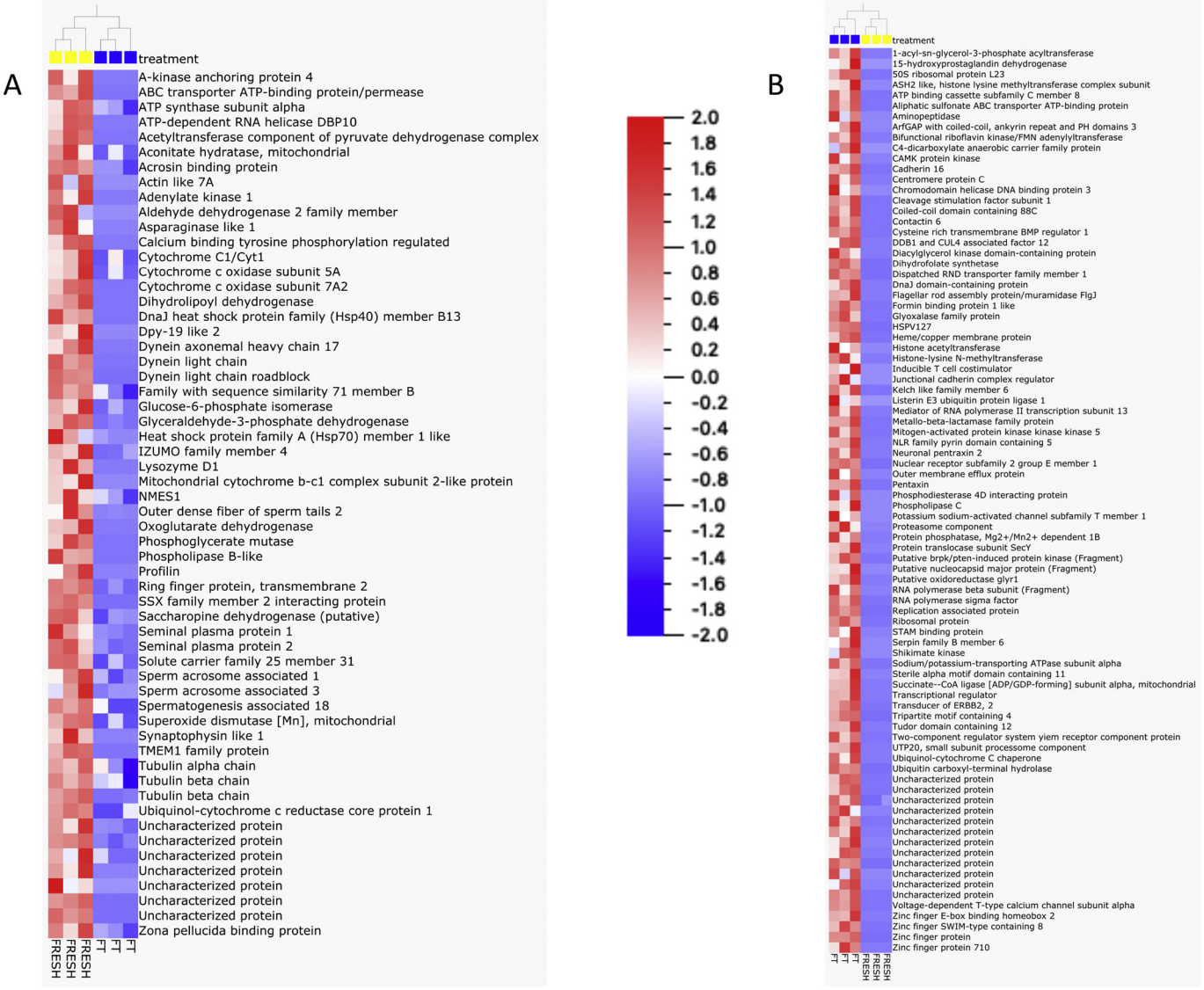

Fig. 6. Heat map showing differences in the relative expression of sperm proteins between fresh and frozen thawed aliquots. A) Proteins showing reduced expression in frozen-thawed subsamples B) Proteins showing increased expression in frozen thawed subsamples ($P < .05$).

subsamples, and that the *β-oxidation of fatty acids* was present in stallion spermatozoa. Interestingly the KEGG pathway *cysteine and methionine metabolism* was enriched in cryopreserved semen, and not in fresh samples. This finding can be explained as an adaptative mechanism to the redox deregulation occurring during the process. Recent research provide evidences that under oxidative stress the stallion spermatozoa may activate glutathione synthesis from cysteine [16,17]. Also, the individual analysis of specific proteins, revealed that the proteins

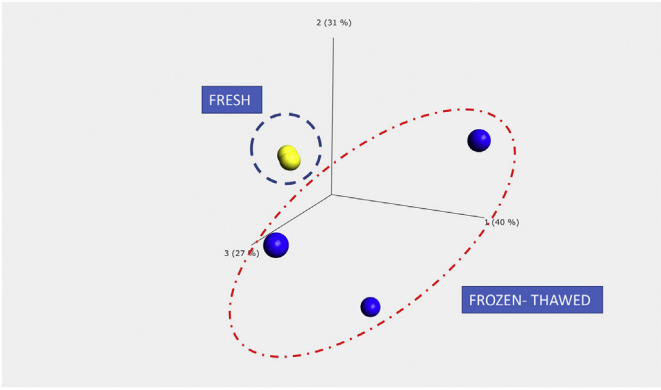

Fig. 7. Three-dimensional Principal Component Analysis (PCA) evaluating differences in the relative quantities of sperm proteins between fresh (yellow) and frozen thawed aliquots (blue).

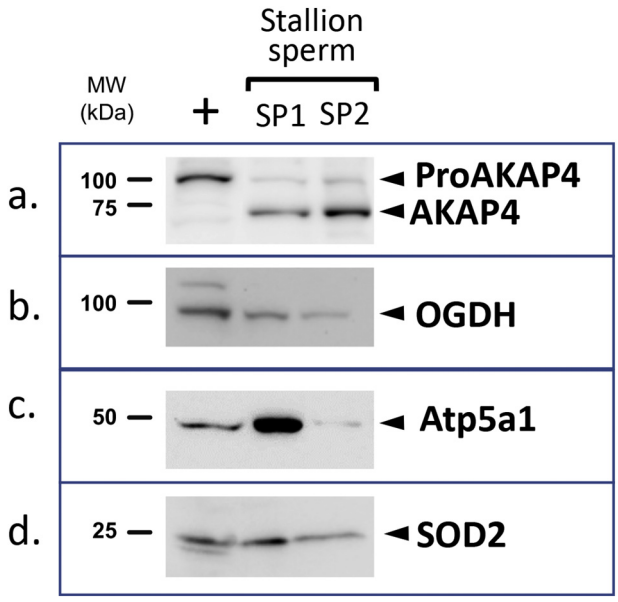

Fig. 8. Representative subset of proteins identified with reduced expression in frozen thawed samples, were validated through western blotting analysis. Fresh sperm lysates from two different stallions were used, and AKAP4 (a), OGDH (b), ATP5A1 (c) and SOD2 (d) identified. Positive controls used were SH-SY5Y cells for AKAP4, Brain lysates for OGDH and Atp5a1, and lung lysates for SOD2.

aldehyde dehydrogenase and *mitochondrial superoxide dismutase* were significantly reduced in the thawed samples. Superoxide dismutase constitutes the first line of defense against oxidative stress [62]; aldehyde dehydrogenase plays a pivotal role in stallion sperm functionality [7], being a key enzyme in detoxication of lipid hydroperoxides such as 4-HNE that are produced in high amounts during cryopreservation [17,18].

The findings reported here are novel and provide an in deep, new, molecular perspective to the understanding of the damage induced by cryopreservation. The predominance of ATP synthases in fresh spermatozoa confirms and supports studies showing the high dependence of stallion spermatozoa of mitochondrial production of ATP through oxidative phosphorylation [2,7,10,11,18,63,64]. Moreover the importance of ATP synthase have been previously reported [6]; inhibition of ATP synthase collapsed sperm membranes and increased ROS production rapidly, leading to sperm death. Moreover, the mitochondrial damage and redox deregulation occurring as consequence of cryopreservation are well documented [5,16–18,24,65–67] and have also been detected in our study. Relative changes of proteins involved in ATP production also confirm this hypothesis, with reduced levels of ATP synthase, and the ADP/ATP antiporter SLC25A31 in frozen thawed samples, interestingly previously reports suggested a role for this antiporter in stallion sperm functionality [68].

Changes reported in the main classes of proteins confirm the mitochondrial impairment and redox deregulation behind cryodamage to spermatozoa. Further confirming this point is the fact that frozen thawed spermatozoa is 2.41 mV per million of spermatozoa more oxidized than fresh samples. Another interesting finding is enriched annotations related to sperm metabolism that were only present in fresh samples. There was a significant enrichment in the KEGG pathways *oxidative phosphorylation, carbon metabolism, glycolysis gluconeogenesis, citrate cycle (TCA Cycle) pyruvate metabolism, and also in fatty acid degradation, butanoate and propanoate metabolism, valine and leucine metabolism, cysteine and methionine metabolism and biosynthesis of amino acids*. Analysis of these pathways confirms previous reports in human [14,15] and stallion spermatozoa [13], showing that spermatozoa can oxidize fatty acids, and also suggest that spermatozoa can use amino acids as source of energy. The use of short chain fatty acids such as propanoate and butyrate as source of energy in spermatozoa deserves further research; these fatty acids can activate pro-survival pathways and improve mitochondrial respiration in colonocytes [69]. Also, the fact that stallion sperm can oxidize amino acids, and particularly the presence of amino acid synthesis deserve further attention. In this regard recent research evidences glutathione synthesis in stallion spermatozoa [17], finding supported by the presence of the *cysteine and methionine metabolism pathway* in the present study. Numerous proteins with oxidoreductase activity were overrepresented in fresh stallion spermatozoa. *Glutathione and glutathione reductase* were present in functional networks of our study confirming previous findings [17] on the importance of this molecule on sperm redox regulation and underlying the importance of redox signaling in the functionality of spermatozoa. Finally, the impairment of cryopreserved spermatozoa can be explained through changes in proteins important for the acrosome reaction and fecundation itself. Relative abundance of the *acrosin binding protein, sperm acrosome associated proteins 1, 3, and 18 and IZUMO family member* 4 were reduced after cryopreservation.

Few studies have addressed the impact of cryopreservation in the mammalian sperm proteome. There are reports in humans [70,71], pigs [72,73] and sheep [74]. There is a recent paper studying the proteome of bull spermatozoa after cryopreservation [75]. However to the best of our knowledge this is the first paper addressing the impact of cryopreservation on stallion spermatozoa, and there is only one previous study addressing the stallion sperm proteome [13]. In accordance with most studies, substantial changes as consequence of cryopreservation were observed, however most studies focus on individual proteins instead of performing enrichment analysis. This fact in addition to the species used in our study, makes comparisons difficult. Nevertheless, both aspects are covered in our study, and some comparison can be done. First the fact that cryopreservation increases the levels of some proteins and reduces others [70,74]. Reduced levels can be easily explained by protein degradation during the procedure; however increased levels are less clearly explained since spermatozoa are considered transcriptionally and translationally silent, but have been also observed in previous studies [70]. It has been proposed that these changes may relate to protein degradation, post translational modifications, and/or alterations in secondary or tertiary structures and translocation to other structures or outside the cell [71]. In any case, an explanation for this phenomenon requires further research. Interestingly, most studies to date also detect changes in mitochondrial proteins involved in metabolism and redox regulation [72,73].

In conclusion, we have provided the first detailed study on how the cryopreservation process impacts the stallion sperm proteome. Although we should make a note of caution since our study involved a limited number of stallions, but our findings identify the metabolic proteome and redoxome as the two key groups of proteins affected by

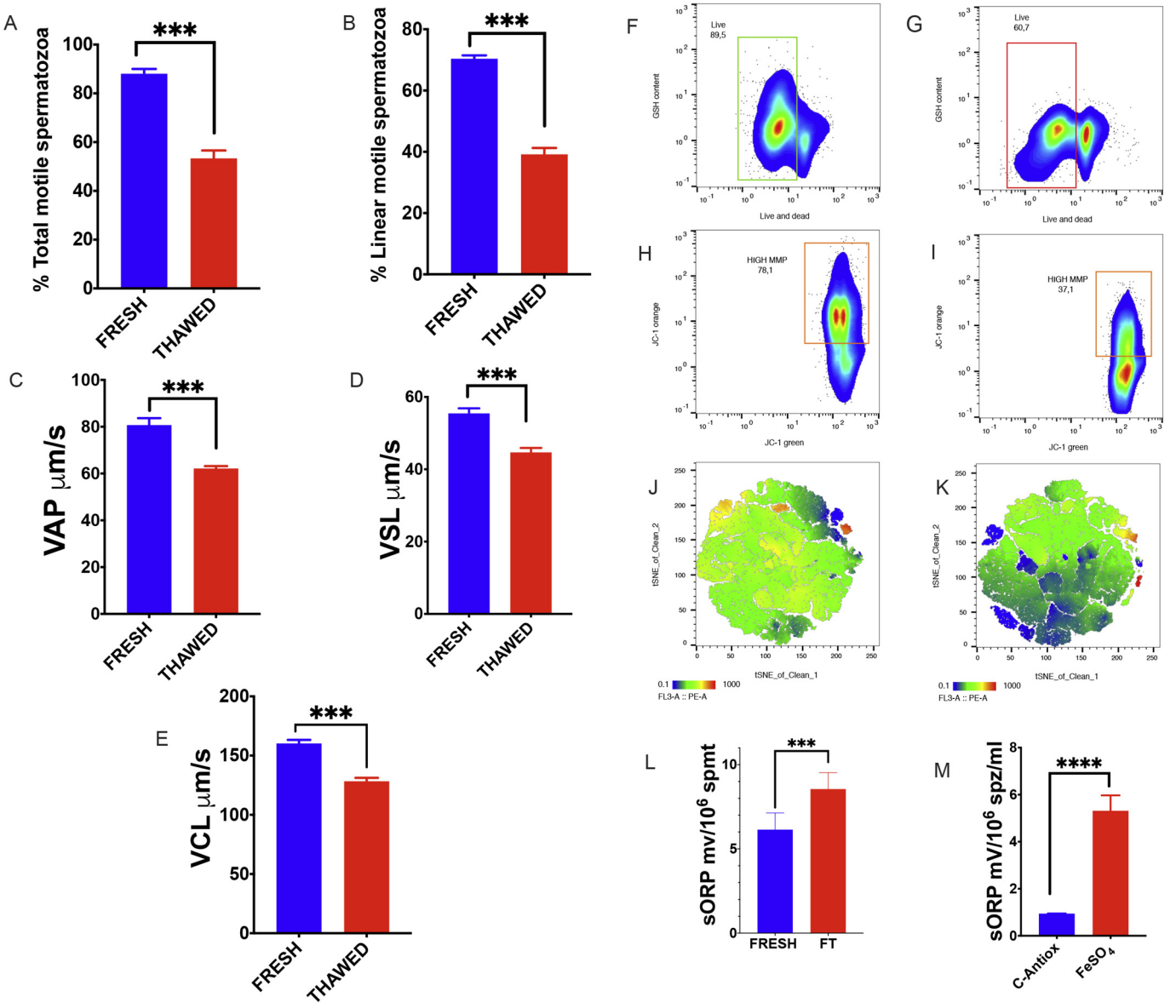

Fig. 9. Effect of cryopreservation on sperm motility, velocities, viability, GSH content mitochondrial membrane potential and steady state redox potential (E_h). Ejaculates were processed and analyzed as described in material and methods. Cryopreservation impacted all the sperm parameters evaluated. A-B) The percentages of total motile and linear motile spermatozoa were lower in frozen thawed aliquots ($P < .001$). C-E) Sperm velocities decreased after cryopreservation ($P < .001$). Cryopreservation also impacted sperm viability F) percentage of live spermatozoa in fresh samples, G) Percentage of live spermatozoa in frozen thawed samples ($P < .01$). Also as seen in G GSH content was reduced in frozen thawed samples ($P < .01$). Mitochondrial activity was particularly impacted by cryopreservation, in H and I the drop in the percentage of spermatozoa showing high mitochondrial membrane potential is depicted ($P < .001$). J-K) t-SNE maps in which each point represent an individual spermatozoa, as seen in K cryopreservation caused a significant decline in the mitochondrial potential, showed as increased dark green and blue areas in the t SNE map in comparison with J. L) Cryopreservation also induced and increase in the steady state redox potential ($P < .001$) M) Positive and negative controls for the oxidation reduction potential assay.

the procedure; also we identified key individual proteins, which levels decreased after cryopreservation with key roles in the acrosome reaction and fertilization itself, that may help to explain the reduced fertility and increased embryo mortality observed with cryopreserved spermatozoa [17,19]. Moreover, this study contributes to detect targets to improve current sperm conservation procedures, and also may provide clues to detect proteins with a direct role in oocyte activation and support early embryo development.

Declaration of Competing Interest

The authors declare that there are no conflicts of interest that could be perceived to prejudice the reported research.

Acknowledgements

The authors received financial support for this study from the Ministerio de Economía y Competitividad-FEDER, Madrid, Spain, grants, AGL2017-83149-R and Junta de Extremadura-FEDER (GR 18008 and IB16030). JMOR holds a PhD grant from the Junta de Extremadura- FEDER (PD 18005), Mérida, Spain. GGPh holds a PhD grant from the Ministry of Science, Madrid, Spain (PRE2018-083354).

Appendix A. Supplementary data

Supplementary data to this article can be found online at https://doi.org/10.1016/j.jprot.2020.103765.

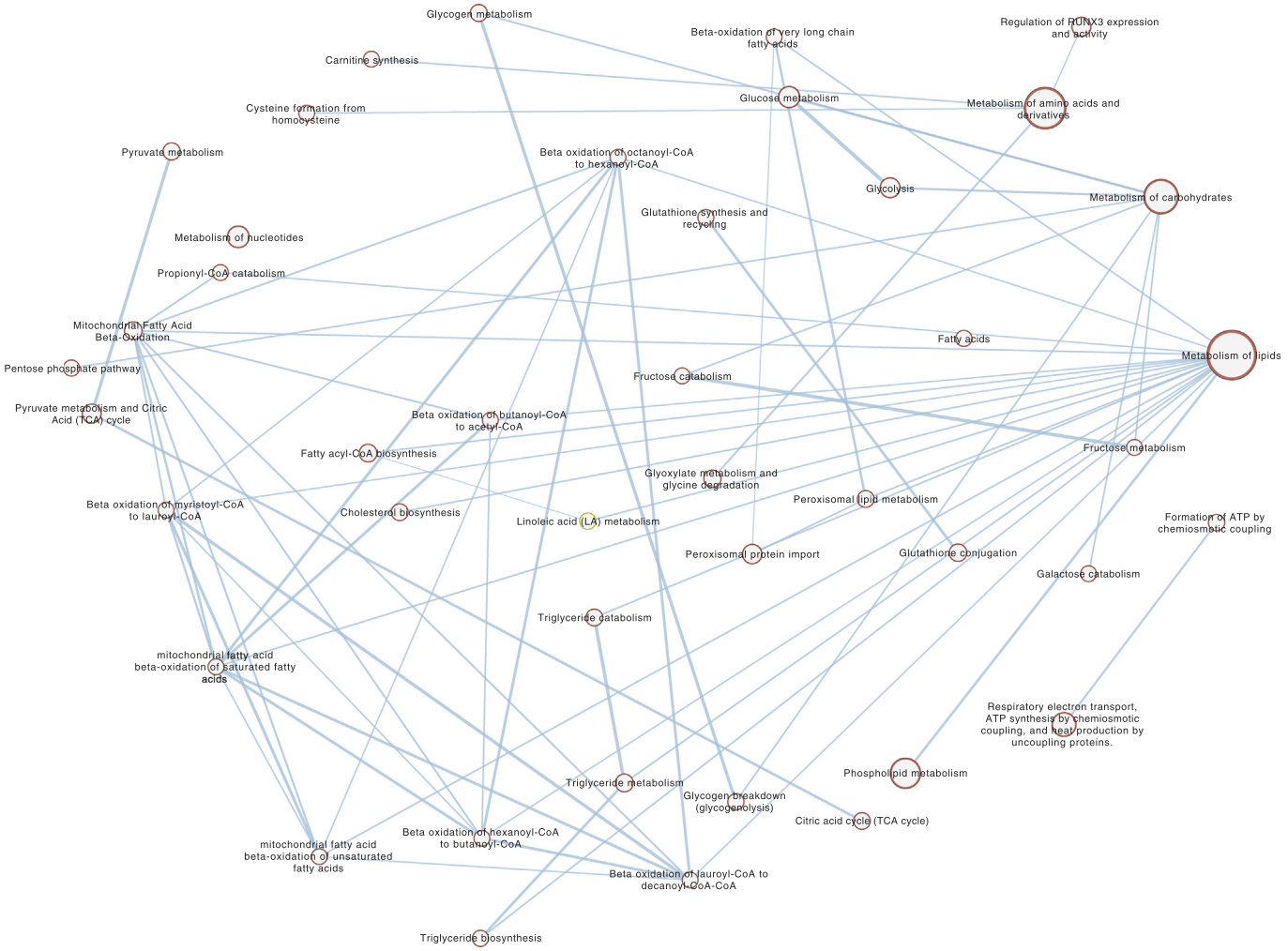

Fig. 10. Enrichment map using g:Profiler, Cytoscape and EnrichmentMap depicting metabolic pathways overrepresented in stallion spermatozoa.

References

[1] A.M. Rodriguez, C.O. Ferrusola, B.M. Garcia, J.M. Morrell, H.R. Martinez, J.A. Tapia, F.J. Pena, Freezing stallion semen with the new Caceres extender improves post thaw sperm quality and diminishes stallion-to-stallion variability, Anim. Reprod. Sci. 127 (1–2) (2011) 78–83.

[2] D.D. Varner, Z. Gibb, R.J. Aitken, Stallion fertility: a focus on the spermatozoon, Equine Vet. J. 47 (1) (2015) 16–24.

[3] S.P. Brinsko, D.D. Varner, Artificial insemination and preservation of semen, Vet. Clin. North Am. Equine Pract. 8 (1) (1992) 205–218.

[4] C. Ortega Ferrusola, P. Martin Munoz, J.M. Ortiz-Rodriguez, L. Anel-Lopez, C. Balao da Silva, M. Alvarez, P. de Paz, J.A. Tapia, L. Anel, A. Silva-Rodriguez, R.J. Aitken, M.C. Gil, Z. Gibb, F.J. Pena, Depletion of thiols leads to redox deregulation, production of 4-hydroxinonenal and sperm senescence: a possible role for GSH regulation in spermatozoa, Biol. Reprod. 101 (2019) 1090–1107.

[5] C. Ortega Ferrusola, L. Anel-Lopez, J.M. Ortiz-Rodriguez, P. Martin Munoz, M. Alvarez, P. de Paz, J. Masot, E. Redondo, C. Balao da Silva, J.M. Morrell, H. Rodriguez Martinez, J.A. Tapia, M.C. Gil, L. Anel, F.J. Pena, Stallion spermatozoa surviving freezing and thawing experience membrane depolarization and increased intracellular Na, Andrology 5 (6) (2017) 1174–1182.

[6] M.P. Davila, P.M. Munoz, J.M. Bolanos, T.A. Stout, B.M. Gadella, J.A. Tapia, C.B. da Silva, C.O. Ferrusola, F.J. Pena, Mitochondrial ATP is required for the maintenance of membrane integrity in stallion spermatozoa, whereas motility requires both glycolysis and oxidative phosphorylation, Reproduction 152 (6) (2016) 683–694.

[7] Z. Gibb, S.R. Lambourne, B.J. Curry, S.E. Hall, R.J. Aitken, Aldehyde dehydrogenase plays a pivotal role in the maintenance of stallion sperm motility, Biol. Reprod. 94 (6) (2016) 133.

[8] Z. Gibb, R.J. Aitken, The impact of sperm metabolism during in vitro storage: the stallion as a model, Biomed. Res. Int. 2016 (2016) 9380609.

[9] R.J. Aitken, Z. Gibb, M.A. Baker, J. Drevet, P. Gharagozloo, Causes and consequences of oxidative stress in spermatozoa, Reprod. Fertil. Dev. 28 (1–2) (2016) 1–10.

[10] Z. Gibb, S.R. Lambourne, J. Quadrelli, N.D. Smith, R.J. Aitken, L-carnitine and pyruvate are prosurvival factors during the storage of stallion spermatozoa at room temperature, Biol. Reprod. 93 (4) (2015) 104.

[11] Z. Gibb, S.R. Lambourne, R.J. Aitken, The paradoxical relationship between stallion fertility and oxidative stress, Biol. Reprod. 91 (3) (2014) 77.

[12] R.J. Aitken, Z. Gibb, L.A. Mitchell, S.R. Lambourne, H.S. Connaughton, G.N. De Iuliis, Sperm motility is lost in vitro as a consequence of mitochondrial free radical production and the generation of electrophilic aldehydes but can be significantly rescued by the presence of nucleophilic thiols, Biol. Reprod. 87 (5) (2012) 110.

[13] A. Swegen, B.J. Curry, Z. Gibb, S.R. Lambourne, N.D. Smith, R.J. Aitken, Investigation of the stallion sperm proteome by mass spectrometry, Reproduction 149 (3) (2015) 235–244.

[14] A. Amaral, J. Castillo, J.M. Estanyol, J.L. Ballesca, J. Ramalho-Santos, R. Oliva, Human sperm tail proteome suggests new endogenous metabolic pathways, Mol. Cell. Proteomics 12 (2) (2013) 330–342.

[15] A. Amaral, J. Castillo, J. Ramalho-Santos, R. Oliva, The combined human sperm proteome: cellular pathways and implications for basic and clinical science, Hum. Reprod. Update 20 (1) (2014) 40–62.

[16] J.M. Ortiz-Rodriguez, F.E. Martin-Cano, C. Ortega-Ferrusola, J. Masot, E. Redondo, A. Gazquez, M.C. Gil, I.M. Aparicio, P. Rojo-Dominguez, J.A. Tapia, H. Rodriguez-Martinez, F.J. Pena, The incorporation of cystine by the soluble carrier family 7 member 11 (SLC7A11) is a component of the redox regulatory mechanism in stallion spermatozoadagger, Biol. Reprod. 101 (1) (2019) 208–222.

[17] C. Ortega-Ferrusola, P. Martin Munoz, J.M. Ortiz-Rodriguez, L. Anel-Lopez, C. Balao da Silva, M. Alvarez, P. de Paz, J.A. Tapia, L. Anel, A. Silva-Rodriguez, R.J. Aitken, M.C. Gil, Z. Gibb, F.J. Pena, Depletion of thiols leads to redox deregulation, production of 4-hydroxinonenal and sperm senescence: a possible role for GSH regulation in spermatozoadagger, Biol. Reprod. 100 (4) (2019) 1090–1107.

[18] M. Plaza Davila, P. Martin Munoz, J.A. Tapia, C. Ortega Ferrusola, C.C. Balao da Silva, F.J. Pena, Inhibition of mitochondrial complex I leads to decreased motility and membrane integrity related to increased hydrogen peroxide and reduced ATP production, while the inhibition of glycolysis has less impact on sperm motility, PLoS One 10 (9) (2015) e0138777.

[19] J. Castillo, M. Jodar, R. Oliva, The contribution of human sperm proteins to the development and epigenome of the preimplantation embryo, Hum. Reprod. Update 24 (5) (2018) 535–555.

[20] M. Codina, J.M. Estanyol, M.J. Fidalgo, J.L. Ballesca, R. Oliva, Advances in sperm

proteomics: best-practise methodology and clinical potential, Exp. Rev. Proteome. 12 (3) (2015) 255–277.
[21] A. Amaral, C. Paiva, C. Attardo Parrinello, J.M. Estanyol, J.L. Ballesca, J. Ramalho-Santos, R. Oliva, Identification of proteins involved in human sperm motility using high-throughput differential proteomics, J. Proteome Res. 13 (12) (2014) 5670–5684.
[22] S. de Mateo, J.M. Estanyol, R. Oliva, Methods for the analysis of the sperm proteome, Methods Mol. Biol. 927 (2013) 411–422.
[23] C. Ortega-Ferrusola, L. Anel-Lopez, P. Martin-Munoz, J.M. Ortiz-Rodriguez, M.C. Gil, M. Alvarez, P. de Paz, L.J. Ezquerra, A.J. Masot, E. Redondo, L. Anel, F.J. Pena, Computational flow cytometry reveals that cryopreservation induces spermptosis but subpopulations of spermatozoa may experience capacitation-like changes, Reproduction 153 (3) (2017) 293–304.
[24] F.J. Pena, M. Plaza Davila, B.A. Ball, E.L. Squires, P. Martin Munoz, C. Ortega Ferrusola, C. Balao da Silva, The impact of reproductive technologies on stallion mitochondrial function, Reprod. Domest. Anim. 50 (4) (2015) 529–537.
[25] J.M. Morrell, B.M. Garcia, F.J. Pena, A. Johannisson, Processing stored stallion semen doses by single layer centrifugation, Theriogenology 76 (8) (2011) 1424–1432.
[26] C. Ortega-Ferrusola, B.M. Garcia, J.M. Gallardo-Bolanos, L. Gonzalez-Fernandez, H. Rodriguez-Martinez, J.A. Tapia, F.J. Pena, Apoptotic markers can be used to forecast the freezeability of stallion spermatozoa, Anim. Reprod. Sci. 114 (4) (2009) 393–403.
[27] S.E. Hall, R.J. Aitken, B. Nixon, N.D. Smith, Z. Gibb, Electrophilic aldehyde products of lipid peroxidation selectively adduct to heat shock protein 90 and arylsulfatase a in stallion spermatozoa, Biol. Reprod. 96 (1) (2017) 107–121.
[28] H. Mi, A. Muruganujan, J.T. Casagrande, P.D. Thomas, Large-scale gene function analysis with the PANTHER classification system, Nat. Protoc. 8 (8) (2013) 1551–1566.
[29] H. Mi, A. Muruganujan, P.D. Thomas, PANTHER in 2013: modeling the evolution of gene function, and other gene attributes, in the context of phylogenetic trees, Nucleic Acids Res. 41 (Database issue) (2013) D377–D386.
[30] U. Raudvere, L. Kolberg, I. Kuzmin, T. Arak, P. Adler, H. Peterson, J. Vilo, Profiler: a web server for functional enrichment analysis and conversions of gene lists (2019 update), Nucleic Acids Res. 47 (W1) (2019) W191–W198.
[31] J. Du, Z. Yuan, Z. Ma, J. Song, X. Xie, Y. Chen, KEGG-PATH: Kyoto encyclopedia of genes and genomes-based pathway analysis using a PATH analysis model, Mol. BioSyst. 10 (9) (2014) 2441–2447.
[32] E. Altermann, T.R. Klaenhammer, PathwayVoyager: pathway mapping using the Kyoto Encyclopedia of Genes and Genomes (KEGG) database, BMC Genomics 6 (2005) 60.
[33] H. Ogata, S. Goto, K. Sato, W. Fujibuchi, H. Bono, M. Kanehisa, KEGG: Kyoto Encyclopedia of genes and genomes, Nucleic Acids Res. 27 (1) (1999) 29–34.
[34] H. Mi, A. Muruganujan, X. Huang, D. Ebert, C. Mills, X. Guo, P.D. Thomas, Protocol update for large-scale genome and gene function analysis with the PANTHER classification system (v.14.0), Nat. Protoc. 14 (3) (2019) 703–721.
[35] J. Reimand, R. Isserlin, V. Voisin, M. Kucera, C. Tannus-Lopes, A. Rostamianfar, L. Wadi, M. Meyer, J. Wong, C. Xu, D. Merico, G.D. Bader, Pathway enrichment analysis and visualization of omics data using g:profiler, GSEA, Cytoscape and EnrichmentMap, Nat Protoc 14 (2) (2019) 482–517.
[36] I.M. Aparicio, P. Martin Munoz, G.M. Salido, F.J. Pena, J.A. Tapia, The autophagy-related protein LC3 is processed in stallion spermatozoa during short-and long-term storage and the related stressful conditions, Animal (2016) 1–10.
[37] C. Ortega-Ferrusola, B. Macias Garcia, V. Suarez Rama, J.M. Gallardo-Bolanos, L. Gonzalez-Fernandez, J.A. Tapia, H. Rodriguez-Martinez, F.J. Pena, Identification of sperm subpopulations in stallion ejaculates: changes after cryopreservation and comparison with traditional statistics, Reprod. Domest. Anim. 44 (3) (2009) 419–423.
[38] M.M. Bradford, A rapid and sensitive method for the quantitation of microgram quantities of protein utilizing the principle of protein-dye binding, Anal. Biochem. 72 (1976) 248–254.
[39] M.E. Skindersoe, S. Kjaerulff, Comparison of three thiol probes for determination of apoptosis-related changes in cellular redox status, Cytometry A 85 (2) (2014) 179–187.
[40] M.E. Skindersoe, M. Rohde, S. Kjaerulff, A novel and rapid apoptosis assay based on thiol redox status, Cytometry A 81 (5) (2012) 430–436.
[41] J. Capek, M. Hauschke, L. Bruckova, T. Rousar, Comparison of glutathione levels measured using optimized monochlorobimane assay with those from ortho-phthalaldehyde assay in intact cells, J. Pharmacol. Toxicol. Methods 88 (Pt 1) (2017) 40–45.
[42] F.J. Pena, A. Johannisson, M. Wallgren, H. Rodriguez-Martinez, Assessment of fresh and frozen-thawed boar semen using an Annexin-V assay: a new method of evaluating sperm membrane integrity, Theriogenology 60 (4) (2003) 677–689.
[43] J.M. Gallardo Bolanos, C.M. Balao da Silva, P. Martin Munoz, A. Morillo Rodriguez, M. Plaza Davila, H. Rodriguez-Martinez, I.M. Aparicio, J.A. Tapia, C. Ortega Ferrusola, F.J. Pena, Phosphorylated AKT preserves stallion sperm viability and motility by inhibiting caspases 3 and 7, Reproduction 148 (2) (2014) 221–235.
[44] P. Martin Munoz, C. Ortega Ferrusola, G. Vizuete, M. Plaz Davila, H. Rodriguez Martinez, F.J. Pena Vega, Depletion of intracellular thiols and increased production of 4-hydroxynonenal that occur during cryopreservation of stallion spermatozoa leads to caspase activation, loss of motility, and cell death, Biol. Reprod. 93 (6) (2015) 1–11.
[45] K. Shekhar, P. Brodin, M.M. Davis, A.K. Chakraborty, Automatic classification of cellular expression by nonlinear stochastic embedding (ACCENSE), Proc. Natl. Acad. Sci. U. S. A. 111 (1) (2014) 202–207.
[46] C. Chester, H.T. Maecker, Algorithmic tools for mining high-dimensional cytometry data, J. Immunol. 195 (3) (2015) 773–779.
[47] J.M. Ortiz-Rodriguez, C. Balao da Silva, J. Masot, E. Redondo, A. Gazquez, J.A. Tapia, C. Gil, C. Ortega-Ferrusola, F.J. Pena, Rosiglitazone in the thawing medium improves mitochondrial function in stallion spermatozoa through regulating Akt phosphorylation and reduction of caspase 3, PLoS One 14 (7) (2019) e0211994.
[48] G. Bobe, T.J. Cobb, S.W. Leonard, S. Aponso, C.B. Bahro, D. Koley, E. Mah, R.S. Bruno, M.G. Traber, Increased static and decreased capacity oxidation-reduction potentials in plasma are predictive of metabolic syndrome, Redox Biol. 12 (2017) 121–128.
[49] A. Agarwal, S. Roychoudhury, K.B. Bjugstad, C.L. Cho, Oxidation-reduction potential of semen: what is its role in the treatment of male infertility? Ther. Adv. Urol. 8 (5) (2016) 302–318.
[50] J. Li, I. Barranco, A. Tvarijonaviciute, M.F. Molina, E.A. Martinez, H. Rodriguez-Martinez, I. Parrilla, J. Roca, Seminal plasma antioxidants are directly involved in boar sperm cryotolerance, Theriogenology 107 (2018) 27–35.
[51] A. Agarwal, D. Durairajanayagam, J. Halabi, J. Peng, M. Vazquez-Levin, Proteomics, oxidative stress and male infertility, Reprod. BioMed. Online 29 (1) (2014) 32–58.
[52] N. Lakpour, R.Z. Mahfouz, M.M. Akhondi, A. Agarwal, H. Kharrazi, H. Zeraati, N. Amirjannati, M.R. Sadeghi, Relationship of seminal plasma antioxidants and serum male hormones with sperm chromatin status in male factor infertility, Syst Biol Reprod Med 58 (5) (2012) 236–244.
[53] T. Mostafa, T. Anis, A. El Nashar, H. Imam, I. Osman, Seminal plasma reactive oxygen species-antioxidants relationship with varicocele grade, Andrologia 44 (1) (2012) 66–69.
[54] S.E. Lewis, E.S. Sterling, I.S. Young, W. Thompson, Comparison of individual antioxidants of sperm and seminal plasma in fertile and infertile men, Fertil. Steril. 67 (1) (1997) 142–147.
[55] V.R. Neagu, B.M. Garcia, A.M. Rodriguez, C.O. Ferrusola, J.M. Bolanos, L.G. Fernandez, J.A. Tapia, F.J. Pena, Determination of glutation peroxidase and superoxide dismutase activities in canine seminal plasma and its relation with sperm quality and lipid peroxidation post thaw, Theriogenology 75 (1) (2011) 10–16.
[56] C. Ortega Ferrusola, L. Gonzalez Fernandez, J.M. Morrell, C. Salazar Sandoval, B. Macias Garcia, H. Rodriguez-Martinez, J.A. Tapia, F.J. Pena, Lipid peroxidation, assessed with BODIPY-C11, increases after cryopreservation of stallion spermatozoa, is stallion-dependent and is related to apoptotic-like changes, Reproduction 138 (1) (2009) 55–63.
[57] F.J. Pena, C. O'Flaherty, J.M. Ortiz Rodriguez, F.E. Martin Cano, G.L. Gaitskell-Phillips, M.C. Gil, C. Ortega Ferrusola, Redox regulation and oxidative stress: the particular case of the stallion spermatozoa, Antioxidants (Basel) 8 (11) (2019).
[58] Y. Perez-Riverol, A. Csordas, J. Bai, M. Bernal-Llinares, S. Hewapathirana, D.J. Kundu, A. Inuganti, J. Griss, G. Mayer, M. Eisenacher, E. Perez, J. Uszkoreit, J. Pfeuffer, T. Sachsenberg, S. Yilmaz, S. Tiwary, J. Cox, E. Audain, M. Walzer, A.F. Jarnuczak, T. Ternent, A. Brazma, J.A. Vizcaino, The PRIDE database and related tools and resources in 2019: improving support for quantification data, Nucleic Acids Res. 47 (D1) (2019) D442–D450.
[59] A.P. Panda, S.C. Roy, D.T. Sakhare, S. Badami, B.C. Divyashree, V.S. Gurupriya, A. Dhali, Reduced cytochrome oxidase activity and increased protein tyrosine phosphorylation of mitochondria-rich fractions of buffalo (Bubalus bubalis) spermatozoa after a cycle of freezing and thawing, Reprod. Fertil. Dev. 31 (10) (2019) 1567–1580.
[60] C.R. Moraes, S. Meyers, The sperm mitochondrion: organelle of many functions, Anim. Reprod. Sci. 194 (2018) 71–80.
[61] A. Swegen, S.R. Lambourne, R.J. Aitken, Z. Gibb, Rosiglitazone improves stallion sperm motility, ATP content, and mitochondrial function, Biol. Reprod. 95 (5) (2016) 107.
[62] W.H. Ibrahim, H.M. Habib, H. Kamal, D.K. St Clair, C.K. Chow, Mitochondrial superoxide mediates labile iron level: evidence from Mn-SOD-transgenic mice and heterozygous knockout mice and isolated rat liver mitochondria, Free Radic. Biol. Med. 65 (2013) 143–149.
[63] C.R. Darr, L.E. Moraes, R.E. Connon, C.C. Love, S. Teague, D.D. Varner, S.A. Meyers, The relationship between mitochondrial DNA copy number and stallion sperm function, Theriogenology 94 (2017) 94–99.
[64] P.H. Hung, M.G. Miller, S.A. Meyers, C.A. VandeVoort, Sperm mitochondrial integrity is not required for hyperactivated motility, zona binding, or acrosome reaction in the rhesus macaque, Biol. Reprod. 79 (2) (2008) 367–375.
[65] I.M. Aparicio, P. Martin Munoz, G.M. Salido, F.J. Pena, J.A. Tapia, The autophagy-related protein LC3 is processed in stallion spermatozoa during short-and long-term storage and the related stressful conditions, Animal 10 (7) (2016) 1182–1191.
[66] F.J. Pena, H. Rodriguez Martinez, J.A. Tapia, C. Ortega Ferrusola, L. Gonzalez Fernandez, B. Macias Garcia, Mitochondria in mammalian sperm physiology and pathology: a review, Reprod. Domest. Anim. 44 (2) (2009) 345–349.
[67] C. Ortega-Ferrusola, Y. Sotillo-Galan, E. Varela-Fernandez, J.M. Gallardo-Bolanos, A. Muriel, L. Gonzalez-Fernandez, J.A. Tapia, F.J. Pena, Detection of "apoptosis-like" changes during the cryopreservation process in equine sperm, J. Androl. 29 (2) (2008) 213–221.
[68] C. Ortega Ferrusola, L. Gonzalez Fernandez, C. Salazar Sandoval, B. Macias Garcia, H. Rodriguez Martinez, J.A. Tapia, F.J. Pena, Inhibition of the mitochondrial permeability transition pore reduces "apoptosis like" changes during cryopreservation of stallion spermatozoa, Theriogenology 74 (3) (2010) 458–465.
[69] D.R. Donohoe, N. Garge, X. Zhang, W. Sun, T.M. O'Connell, M.K. Bunger, S.J. Bultman, The microbiome and butyrate regulate energy metabolism and autophagy in the mammalian colon, Cell Metab. 13 (5) (2011) 517–526.
[70] O.A. Bogle, K. Kumar, C. Attardo-Parrinello, S.E. Lewis, J.M. Estanyol, J.L. Ballesca,

R. Oliva, Identification of protein changes in human spermatozoa throughout the cryopreservation process, Andrology 5 (1) (2017) 10–22.
[71] S. Wang, W. Wang, Y. Xu, M. Tang, J. Fang, H. Sun, Y. Sun, M. Gu, Z. Liu, Z. Zhang, F. Lin, T. Wu, N. Song, Z. Wang, W. Zhang, C. Yin, Proteomic characteristics of human sperm cryopreservation, Proteomics 14 (2–3) (2014) 298–310.
[72] C. Perez-Patino, I. Barranco, J. Li, L. Padilla, E.A. Martinez, H. Rodriguez-Martinez, J. Roca, I. Parrilla, Cryopreservation differentially alters the proteome of Epididymal and ejaculated pig spermatozoa, Int. J. Mol. Sci. 20 (7) (2019).
[73] C. Perez-Patino, J. Li, I. Barranco, E.A. Martinez, H. Rodriguez-Martinez, J. Roca, I. Parrilla, The proteome of frozen-thawed pig spermatozoa is dependent on the ejaculate fraction source, Sci. Rep. 9 (1) (2019) 705.
[74] T. Pini, J.P. Rickard, T. Leahy, B. Crossett, X. Druart, S.P. de Graaf, Cryopreservation and egg yolk medium alter the proteome of ram spermatozoa, J. Proteome 181 (2018) 73–82.
[75] O. D'Amours, G. Frenette, S. Bourassa, E. Calvo, P. Blondin, R. Sullivan, Proteomic markers of functional sperm population in bovines: comparison of low- and high-density spermatozoa following cryopreservation, J. Proteome Res. 17 (1) (2018) 177–188.